Chemie der Erde 77 (2017) 183–194

Contents lists available at ScienceDirect

Chemie der Erde

journal homepage: www.elsevier.de/chemer

Petrogenesis and geochemical characteristics of plagiogranites from Naga Ophiolite Belt, northeast India: Fractional crystallization of MORB-type magma

Ranjit Nayak[a,*], B.V. Rao[b]

[a] Department of Earth and Atmospheric Sciences, NIT, Rourkela 769008, India
[b] Department of Geology, Nagaland University, Kohima, Nagaland 797001, India

ARTICLE INFO

Article history:
Received 11 March 2016
Received in revised form 31 October 2016
Accepted 7 November 2016
Editorial handling - Dr. Dewashish Upadhyay

Keywords:
Petrology
Geochemistry
Plagiogranite
Naga Ophiolite Belt (NOB)
Fractional crystallization

ABSTRACT

The Naga Ophiolite Belt is a part of the Naga-Arakan-Yoma flysch trough that occurs along the Indo-Myanmar border. It is represented by peridotites, mafic-ultramafic cumulates, mafic volcanics, mafic dykes, plagiogranites, pelagic sediments and minor felsic to intermediate intrusives. Minor plagiogranites, gabbros and thin serpentinite bands occur juxtaposed near Luthur, with the slate-phyllite-metagreywacke sequence (Phokpur Formation) adjacent to the contact. The development of tonalites, trondhjemites and diorites in the oceanic crust, which is grouped as plagiogranites, offers an opportunity to study the process of formation of silicic melts from mafic crust. Plagiogranites from Naga Ophiolite Belt contains moderate SiO_2 (51.81–56.71 wt.%), low K_2O (0.08–1.65 wt.%) and high Na_2O (4.3–5.03 wt.%). The Naga Ophiolite Belt plagiogranites like ocean-ridge granites contain low K_2O, high Na_2O and CaO. The rocks investigated from Naga Ophiolite Belt contain TiO_2 concentrations above the lower limit for fractionated Mid Oceanic Ridge Basalt which is above 1 wt% of TiO_2 and the ternary plots of A ($Na_2O + K_2O$) F(FeO^T) M(MgO) and TiO_2-K_2O-$SiO_2/50$ indicate that the plagiogranite are tholeiitic in character and gabbro samples are calc-alkaline in nature. The plagiogranites are enriched in Rb, Ba, Th, U, Nb and Sm against chondrite with negative anomalies on Sr and Zr whereas Y and Yb are depleted to Mid Oceanic Ridge Basalt. The chondrite normalized REE patterns of the plagiogranite display enrichments in LREE (La_N/Sm_N: 2.37–3.62) and flat HREE (Eu/Eu*: 0.90–1.06). The Mid Oceanic Ridge Basalt normalization of gabbro is characterized by strong enrichment of LILE like Ba and Th. The REE pattern is about 50–100 times chondrite with slight enrichment of LREE (La_N/Sm_N = 2.21–3.13) and flat HREE (Eu/Eu*: 0.94–1.19). The major-element and trace element data of the NOB plagiogranites and their intrusive nature with host gabbroic rock suggest that the plagiogranites were produced by fractional crystallization of basaltic parental magmas at Mid Oceanic Ridge.

1. Introduction

Ophiolite section is an oceanic magmatic complex which comprises of ultramafic rocks at the bottom like serpentinized harzburgite, lherzolite and dunite, overlain by gabbroic rocks which form beneath extrusive rocks, such as basalts, with or without sheeted dykes and deep-sea pelagic sediments at the top (Robertson, 2002). Ophiolites preserve momentous evidences for tectonic and magmatic processes from rift-drift through accretionary and collisional stages of continental margin evolution in various tectonic settings. Ophiolites of the world might have originated at different tectonic settings, either at the mid-ocean ridge (MOR) settings characterized by fertile mantle and Al-rich spinel or at the suprasubduction-zone (SSZ) environments affinity marked by refractory mantle character and Cr-rich spinel (Pearce et al., 1981; Dick and Bullen, 1984).

World's best-known ophiolites (on-land remnants of oceanic lithosphere) have petrologic and geochemical characteristics that suggest the formation above a subduction zone, an environment of formation known as a suprasubduction-zone environment (e.g., Pearce et al., 1984). In addition, many suprasubduction-zone ophiolites appear to have been formed shortly after the initiation of subduction in a nascent arc environment, where oceanic crust formed in concert with significant extension over a subducting slab that was rolling back (Stern and Bloomer, 1992). Most ophiolite researchers ascribe to the tectonic model of Stern and Bloomer

* Corresponding author.
E-mail address: nayak.ranjit213@gmail.com (R. Nayak).

http://dx.doi.org/10.1016/j.chemer.2016.11.001
0009-2819/

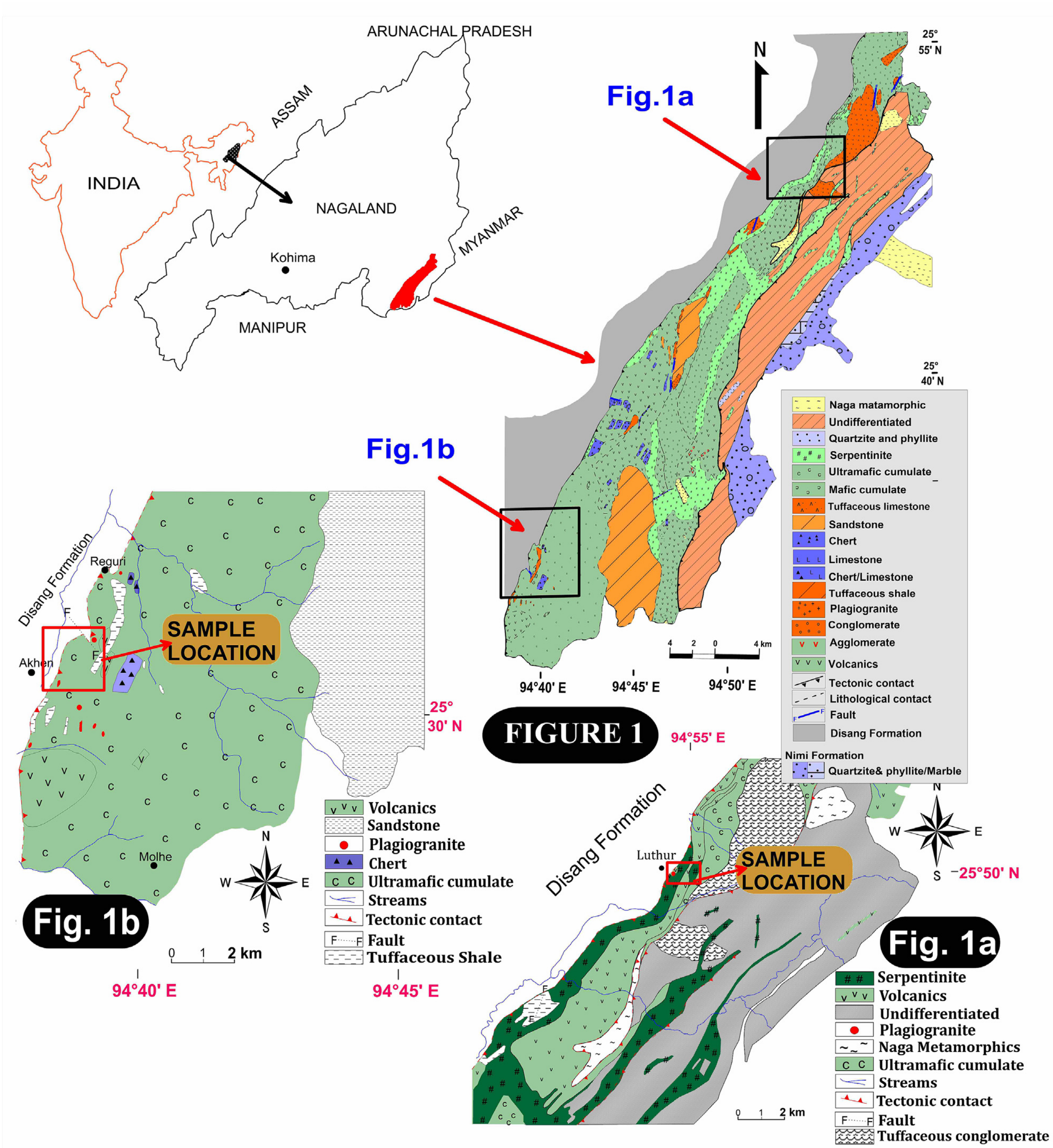

Fig. 1. JPG: Simplified geological map of Naga Ophiolite Belt (NOB), (a) Geological map of northern part of Naga Ophiolite Belt; (b) Geological map of southern part of Naga Ophiolite Belt, Nagaland, Northeast India (after GSI Memoirs vol.119, 1986).

(1992) or variations on that model (e.g., Shervais, 2001; Dilek and Flower, 2003), in which emplacement of the suprasubduction-zone ophiolite takes place over the same subduction zone above which the ophiolite formed. In recent years the study of ophiolites has played an important role in better understanding the overall process of mid-ocean ridge and subduction zone, mantle dynamics, magma chamber processes, fluid-rock interactions in oceanic lithosphere, the role of plate tectonics and plume tectonics in crustal evolution. Ophiolites preserve information about the chemistry and spreading of the oceanic crust that formed earlier to orogenesis (Shervais, 2001; Schroetter et al., 2003; Tremblay et al., 2009) and also record the nature and duration of the tectonic process by which oceanic lithosphere is emplaced onto a continental margin (Tremblay et al., 2011).

The term ‘plagiogranite’ describes a leucocratic rock made primarily of plagioclase and quartz, with minor ferromagnesian minerals, virtually devoid of K-feldspar and with very low bulk K_2O typically around 0.2% (Coleman and Peterman, 1975; Amri et al., 1996; Koepke et al., 2007). Small-volume of felsic magmatic rocks associated with ophiolitic complexes has compositions ranging from granite through trondhjemite and tonalite to diorite and are collectively referred to as oceanic plagiogranites (Coleman and Peterman, 1975; Aumento, 1969; Casey, 1997; Silantyev, 1998; Dick et al., 2000; Koepke et al., 2004). Normally, plagiogranites occur as intrusive bodies of various sizes and forms in the upper portions of the plutonic ophiolite sequence and are related with layered or massive gabbros. Three different processes have been suggested for the origin and development of plagiogranites in the oceanic environment. The formation of oceanic plagiogranite has been attributed primarily to either 1) extreme fractional crystallization of a mantle melt (Coleman and Peterman, 1975; Coleman and Donato, 1979; Pallister and Knight, 1981) e.g. like Saikaraman Ophiolite, Turkey (Floyd et al., 1998); Evros Ophiolite, Greece (Bonev and Stampfli, 2009); Nain Ophiolite (Razaei et al., 2012), or 2) partial melting of hydrated mafic crust (Gerlach et al., 1981; Spulber and Rutherford, 1983) as evidence from Canyon Ophiolite (Gerlach et al., 1981), Troodos Ophiolite (Gillis and Coogan, 2002) and 3) under certain conditions, as immiscible liquids coexisting with mafic melts (Philpotts, 1976; Dixon and Rutherford, 1979); as recorded in Andaman Ophiolite (Shastry et al., 2001). Many supportive evidences and arguments from field observations and melting experiments, for the partial melting were given by the recent study of Grimes et al., 2013. However, the most common process of formation of plagiogranites in the ophiolites is fractional crystallization (Gerlach et al., 1981, and the references there in). It is obvious that a single process is not responsible for the formation of plagiogranites but a combination of two or more processes. Generally felsic/intermediate rocks with a similar chemistry and petrography to plagiogranites are also a relatively common occurrence in modern, and analogous, ancient oceanic settings such as mid-ocean ridges (e.g. Indian Ocean Ridge, Engel and Fisher, 1975), island arcs (e.g. Oman, Alabaster et al., 1982; Canyon Mountain, Gerlach et al., 1981) and back-arc basins (e.g. Bay of Islands, Malpas, 1979; S. Chile, Saunders et al., 1979). Plagiogranites in ophiolites have received less attention than volcanic rocks and sheeted dykes.

Naga Ophiolite Belt (NOB) is exposed as an arcuate belt (Fig. 1) between the Disang Formation to the west and the Nimi Formation to the east of the belt. The ophiolites have tectonic contacts on either side with evidence of their transport into and onto the Disang flysch and, in turn have been over-ridden by the Nimi Formation. Parts of the ophiolites of numerous sizes are arranged in NE-SW/N-S trending 'en echelon' outlines with parallel to sub-parallel tectonic interrelations. Although they are not preserved in a sequential order typical of other ophiolite sections in the Tethyan domain (e.g. Semail, Oman Mountains), it is obvious from field oddity that a systematic order might have existed prior to their emplacement. The belt composed of a range of Mesozoic and Cenozoic rocks that originated in the India-Myanmar convergent plate boundary. These rocks do not constitute a continuing sheet, but made up of units randomly put together along faults or they consist of lensoid slices interbedded with Disang Group (Bhattacharjee, 1991).

Plagiogranites in NOB are very poorly studied and no detail work has been carried out by any agency or individual earlier and their origin is not clear. Therefore, the present study aims to characterize the petrography, whole-rock major and trace element geochemistry with an objective to decipher the genesis and possible tectonic environment of formation of plagiogranite and also compare the relation of plagiogranite with the gabbroic rocks in NOB.

2. Geological setting

The belt is exposed along the eastern part of Nagaland with tectonic contacts on either side. Ophiolite belt and associated rocks of Nagaland are broadly classified into three distinct tectonostratigraphic units, viz., (1) the Nimi Formation consisting of low to medium-grade accretionary wedge metasediments of possible Mesozoic age, (2) the Naga Ophiolite Belt and (3) the Disang Formation consisting of a thick pile of folded Late Cretaceous-Eocene flysch-type sediments (Ghose et al., 2014).

2.1. Nimi formation

The low-grade metasediments of Nimi Formation probably representing the accretionary wedge, and its underlying Naga Metamorphics rocks is thrusted over the NOB from the east. The formation consists of phyllite, limestone, feldspathic quartzite and quartz sericite schist. The sequence is folded in the form of a major NNE trending overturned anticline. Extensive occurrence of limestone about 140–220 m thick has been noted with the development of stalactites and stalagmites (Agrawal and Ghose, 1986). Presence of mylonitic limestone showing flattened quartz and carbonates suggests its formation under extreme pressure as a result of overthrusting (Ghose et al., 2014).

2.2. Ophiolite belt

The NOB located at the Indo-Burman orogenic belt is a rootless block covering nearly 1000 km^2 with general trend of NNE-SSW. It comprises of dismembered and imbricated sheets of mantle derived serpentinised peridotite tectonite (dunite–harzburgite–lherzolite), mafic-ultramafic cumulates (peridotite–norite–gabbro norite–gabbro–hornblende gabbro plagiogranite–anorthosite), minor dolerite, volcanics and volcanoclastics dominated by basalt and spilite with intrusive felsic veins, and marine sediments containing radiolaria (Agrawal and Kacker, 1980; Chattopadhyay et al., 1983; Agrawal and Ghose, 1986; Venkataramana et al., 1986; Ghose and Agrawal, 1989; Ghose et al., 2010). They are intermingled with oceanic sediments like chert, limestone and greywacke with minor intrusives. The associated pelagic sediments include chert and limestone that are often inter-bedded with the volcanics. The ultramafics are the predominant rock type of the belt. The sheeted dykes, which are considered as important components in ophiolitic complexes, are absent (Singh et al., 2016). The cumulate mafic and ultramafic rocks form an intermediate zone between upper mantle peridotites and volcanics of the oceanic crust (Ghose et al., 2010).

2.3. Disang formation

The Disang Group of rocks is the oldest of the Tertiary succession of Nagaland. They occur between the Ophiolite complex and the Haflong-Disang Thrust. The lower contact of this Group is not exposed whereas it conformably passes upward into the Barail Group. They comprise dark to black carbonaceous and ferruginous concretionary shales with thin beds of siltstone and sandstone. The Disangs are divided into two formations—the Lower and Upper. The Lower Disang is made up of shale intercalated with thin flaggy sandstone while the Upper Disang has a proportionately greater volume of sandstone. The thickness varies between 2000 m to over 3000 m. The rocks have yielded Cretaceous fauna from the lower part and late Eocene *Nummulites* from the upper part. The Disang Group is interpreted to have been deposited as deep sea fans. The NE-SW contact between the ophiolite belt and Disang Flysch in the west is marked by brecciation, silicification, fault gauge, ferrugination and intermixing of litho-units. The Disang Flysch is an approximately 3000-m thick, typical allochthonous turbidite sequence representing trench deposits derived from the hinterlands of the northeastern part of the Indian shield of Proterozoic age (Shillong Plateau and Mikir Hills Massif) and the Sino–Myanmar highlands. It is dominantly composed of shale, slate, phyllite, and schist with rare fossils at the base, passing upward into relatively coarser and thicker sandstone, calcareous shale and olistromal limestone rich in microfauna to the south in Manipur

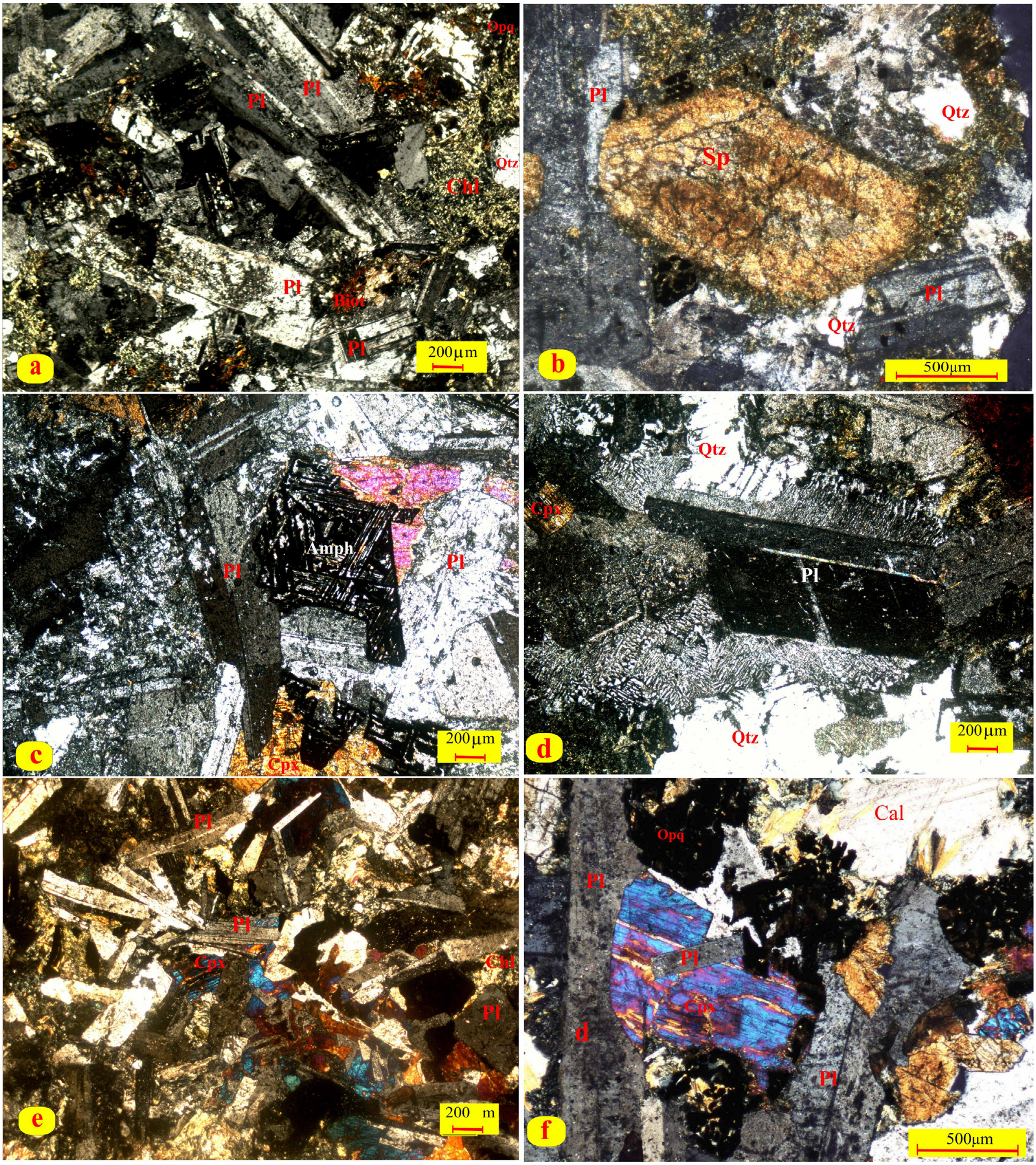

Fig. 2. JPG: Photomicrographs of NOB plagiogranites and gabbros showing (a) hypidiomorphic texture with laths of plagioclase and sericite replacing plagioclase, (b) occurrence of titanite (sphene) along with plagioclase, quartz and opaques (c) corrosion of hornblende along the cleavage plane, (d) micrographic intergrowths of quartz and plagioclase and vermicular blebs of quartz within the plagioclase crystal. (e) Photomicrograph of NOB gabbro showing intergranular texture of plagioclase, pyroxenes and opaques (f) poikilitic texture observed in gabbro. Abbreviations: Pl-plagioclase; Cpx-clinopyroxene; Biot-biotite; Chl-Chlorite; Qzt-quartz; Sp-Sphene; Amp-Amphibole; Cal-Calcite; Opq-opaque.

3. Field relations and petrography

Plagiogranite occurs as intrusive bodies in the mafic and ultramafic cumulates and mafic volcanics in various localities in the study area. Plagiogranite occurs as an elongated body, with a maximum length of about 180 m and width of 100 m, within fractured basalt (Fig. 1a). Minor plagiogranites, gabbros and thin serpentinite bands occur juxtaposed along with the slate-phyllite-metagreywacke sequence (Phokpur Formation) adjacent to the contact. The trends of these intrusives are conformable with the major joints and fractures in the area (NNE-SSW and EW). Southern part of the NOB at Reguri (Fig. 1b), the plagiogranite display both intrusive as well as gradational relation with the gabbro. But there is no chilled margin or any baking effect visible in the wall rocks. Calcite veins were found intruded into the plagiogranites where a number of cavities formed on the exposures. They also occur as

Table 1
Major oxides, trace and REE composition of plagiogranite from NOB. (Sample No: NOL5, 7, 14, 20 and NOR27 are intruded into basalt; Sample No: NOL15,16 and NOR29 are intruded into gabbro; Sample No: NOR9 and NOR11 are intruded into serpentinite).

Sample	NOL5	NOL7	NOL14	NOL15	NOL16	NOL20	NOR9	NOR11	NOR27	NOR29
SiO_2	54.78	56.71	52.22	51.87	51.98	52.25	53.01	52.55	52.43	51.81
TiO_2	1.5	1.24	1.63	1.44	1.74	1.69	1.23	1.83	1.33	1.76
Al_2O_3	13.86	14.47	13.68	14.11	14.14	14.72	14.35	13.42	13.75	13.28
Fe_2O_3t	12.08	11.18	13.35	14.57	13.33	13.02	13.25	12.74	13.21	13.37
MnO	0.2	0.18	0.18	0.21	0.19	0.23	0.19	0.18	0.17	0.17
MgO	2.26	1.74	3.11	3.01	3.29	3.12	3.27	3.26	4.89	5.15
CaO	4.18	4.35	4.13	4.06	5.07	4.23	5.67	5.57	3.26	3.65
Na_2O	5.03	4.3	4.43	4.46	4.7	4.67	4.68	4.81	4.39	4.37
K_2O	0.86	1.65	0.79	0.25	0.77	0.65	0.29	0.19	0.11	0.08
P_2O_5	0.49	0.45	0.55	0.5	0.43	0.21	0.42	0.41	0.79	0.41
LOI	3.01	2.42	4.22	4.10	3.23	4.27	2.46	4.34	3.93	4.50
Total	98.25	98.69	98.29	98.58	98.87	99.06	98.82	99.3	98.26	98.55
Mg#	30.4	26.6	35.2	32.5	36.5	35.8	36.5	37.4	46.3	47.3
Ba	432	662	449	287	375	345	430	175	396	299
Cr	64	92	38	67	46	56	58	71	120	72
V	77	66	92	78	147	230	80	159	145	138
Sc	29	25	34	36	32	30	33	34	37	36
Co	11	10	21	15	24	25	20	28	26	31
Ni	54	56	55	54	60	65	58	56	69	57
Cu	24	24	32	28	50	70	24	36	46	40
Zn	143	152	74	123	121	134	150	149	148	175
Ga	30.12	29.69	30.94	32.02	28.72	29.3	30.94	28.24	25.99	31.79
Pb	4.9	4.7	4.5	5.1	5.14	5.1	4.8	4	5.2	4.8
Th	6.82	8.91	6.59	9.21	6.92	6.35	7.23	6.3	6.88	6.95
Rb	22	45	22	8	20	24	20	5	5	2
U	0.91	1.06	0.89	0.8	0.87	0.91	0.8	0.79	0.8	0.79
Sr	177	360	247	220	183	170	178	134	372	365
Y	47	47	47	47	40	48	47	38	42	41
Zr	285	280	270	290	235	220	280	213	201	232
Nb	58.6	58	55.7	59.6	48.67	42.23	40.23	41.1	40.6	49.7
La	28.2	48.5	43.6	48.3	20	26.2	47.3	33	18.6	27.2
Ce	54	84.9	82.1	82.3	37	55	82.3	60.5	33.9	50.7
Pr	6.5	9.7	9.4	9.5	5.5	5.7	9.2	7.5	4.5	5.9
Nd	26.2	37.4	36.8	37.5	16.5	27.3	38.4	28.9	16.34	22.5
Sm	6.3	8.42	8.64	8.42	5.3	6.2	8.23	7.02	4.23	4.84
Eu	2.11	2.82	2.64	2.61	1.5	2.1	2.59	2.3	1.5	1.7
Gd	7.02	8.96	9.42	8.72	4.9	7.2	8.5	7.4	4.45	5.31
Tb	1.08	1.33	1.41	1.31	0.9	1.5	1.23	1.25	0.7	0.8
Dy	6	7.12	7.88	6.81	4.25	7	7	5.63	3.62	4.32
Ho	1.12	1.49	1.45	1.37	0.8	1.2	1.47	1.33	0.8	0.82
Er	2.68	3.52	3.43	3.17	1.7	2.58	3.26	2.9	1.7	2.02
Tm	0.37	0.5	0.48	0.45	0.28	0.46	0.43	0.4	0.3	0.28
Yb	2.23	3.03	2.89	2.57	1.43	2.4	2.56	2.34	1.5	1.74
Lu	0.32	0.41	0.42	0.36	0.33	0.4	0.39	0.3	0.21	0.24
ΣREE	144.13	218.1	210.56	213.39	100.39	145.24	212.86	160.77	92.35	128.37
La_N/Sm_N	2.82	3.62	3.17	3.61	2.37	2.66	3.62	2.96	2.77	3.54
La_N/Yb_N	8.53	10.79	10.17	12.67	9.43	7.36	12.46	9.51	8.36	10.54
Eu/Eu^*	0.97	0.99	0.89	0.93	0.90	0.96	0.95	0.98	1.06	1.03
A/CNK	0.82	0.87	0.88	0.94	0.80	0.92	0.78	0.06	1.04	0.95

slices within the Disang shale near by a stream. Plagiogranite found in the study area are mostly leucocratic and show felsic and mafic ratio in variable proportions and these rocks show plagioclase laths forming an intergranular texture with mafic minerals.

3.1. Plagiogranites

Plagiogranites from the study area are medium to coarse grained, showing variation in the mafic to felsic mineral abundances across the outcrops. The plagiogranites are essentially made up of plagioclase, clinopyroxene, ±orthopyroxene, amphibole, apatite, less quartz, biotite, carbonates (calcite), opaques and secondary chlorite. These rocks show wide variation in texture from granophyric to hypidiomorphic. But intergranular to hypidiomorphic texture is common. Plagioclase is the most dominant mineral, which are partially to completely altered and are mostly tabular, euhedral to subhedral grains with occasional zoning. The majority of the plagioclase fall within the albitic composition and are mostly twinned on simple albite law. Plagioclase laths form the framework with interstitial spaces filled up by mafics and chlorite (Fig. 2a) which are usually bent and sometimes crushed within a matrix of quartz and sericite. Clouding of the plagioclases is due to sericitisation which is a common feature. Saussuritisation is observed towards the core of the plagioclase crystal with profuse calcite. Secondary mineralization comprises mainly chlorite, epidote, quartz, subordinate amounts of calcite and sphene (titanite) (Fig. 2b).

Quartz invariably forms as an anhedral, partly enclosing in earlier feldspar and also occurs as interstitial grains. Primary mafic phases such as biotite and amphibole are rarely preserved and commonly replaced by chlorite. Hornblendes mostly occur as corroded, prismatic grains, which are partly altered to chlorite and epidote especially along grain boundaries and fracture planes. Biotite occurs in small amounts as subhedral to interstitial masses and partly altered to chlorite and iron oxides. Apatite occurs as small prisms with normal characters. Opaque minerals are abundant represented by ilmenite and magnetite. They occur as both replacement along cleavage planes of hornblendes (Fig. 2c) and ex-solution products in clinopyroxenes, largely increasing in abundances with a high presence of both the primary and secondary ferromagnesian minerals. The plagiogranites is characterized by the occurrence of

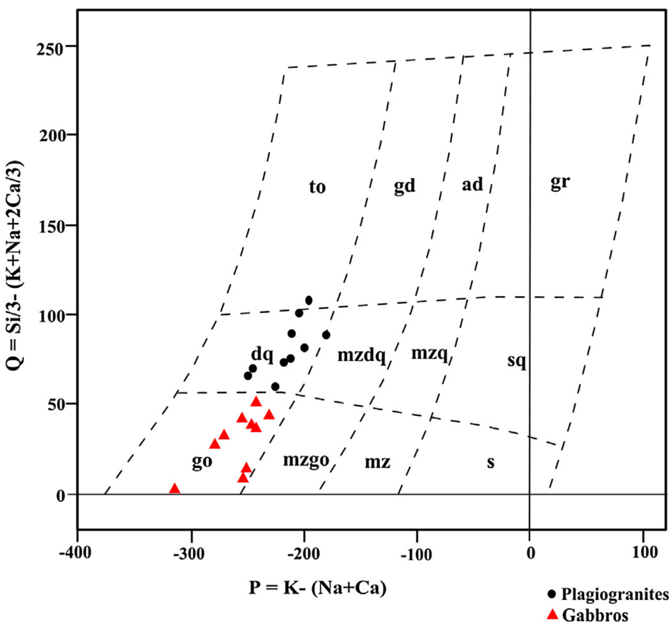

Fig. 3. TIF: P-Q Diagram of NOB plagiogranite (after Debon and Le Fort, 1983) go:gabbro, diorite, anorthosite; mzgo: monzogabbro, monzodiorite; mz:monzonite; s: syenite; dq:qtz diorite, qtz gabbro, qtz anorthosite; mzdq:qtz monzodiorite, qtz monzogabbr; mzq:quartz monzonite; sq:quartz syenite, to tonalite, trondhjemite; gd:granodiorite, granogabbro; ad:adamellite; gr:granite.

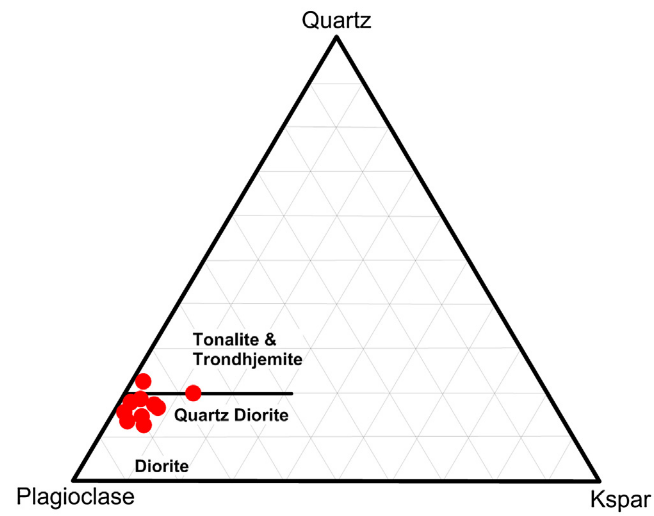

Fig. 4. TIF: Normative quartz-plagioclase-orthoclase ternary diagram showing divisions of diorite (<5% quartz), quartz diorite (5%–20% quartz) and tonalite-trondhjemite (>20% quartz); note that the NOB plagiogranites are largely quartz diorite.

interstitial vermicular and micrographic intergrowths of quartz and plagioclase feldspar (Fig. 2d). The occurrence of secondary minerals like chlorite, muscovite and calcite indicates that the rocks have undergone greenschist metamorphism.

3.2. Gabbros

The gabbros form NOB are mesocratic, massive, fine to coarse grained. In coarse grain rocks, feldspar grains are prominent and appear as dirty white in colour and in fine to medium grained gabbroic rocks display well developed layering with preferred orientation by plagioclase laths. Gabbro samples from study area are made up of various proportions of plagioclase, clinopyroxene, olivine, orthopyroxene, hornblende and opaques having hypidiomorphic texture with large, subhedral, partially to completely saussuritised plagioclase which encloses resorbed oikocrysts of clinopyroxene, orthopyroxene, hornblende and opaque. The observed textures are porphyritic, poikilitic, ophitic, cumulus, mesh, inequigranular and interlocking. In most thin sections the minerals are optically strain free (Fig. 2e). Hornblende is rimmed by secondary chlorite and magnetite. They have a hypidiomorphic texture with an interlocking mosaic of subhedral plagioclase, clinopyroxene, olivine, and rare orthopyroxene.

Clinopyroxene occurs as subhedral to euhedral crystals intergrown with plagioclase (Fig. 2f), or it is involved within the primary greenish-brown amphibole. Secondary actinolite replaces pyroxene rims, or is present in the interstices after primary amphibole. Both plagioclase and pyroxene are poikilitically enclosed in primary amphibole. The crystallization order is plagioclase → plagioclase + clinopyroxene → amphibole. The gabbro has experienced a variable overprint of ocean floor hydrothermal alteration and/or weak greenschist metamorphism.

4. Analytical techniques

The bulk rock (major oxides and trace elements) analyses for 21 representative samples of plagiogranites and gabbros were determined by Wavelength-dispersive X-ray Fluorescence (XRF) Spectrometer (WDXRF, Siemens SRS 3000). The rare earth element (REE) concentrations of the studied samples were analyzed by Inductively Coupled Mass Spectrometry (ICP-MS, ELAN DRC-E, Perkin Elmer). Both the major oxides and trace elements were analyzed at the Wadia Institute of Himalayan Geology (WIHG), Dehradun India. The standard used for XRF and ICPMS is JG-2 (Japan). For XRF analyses the analytical precision is within ±2%–3% for major elements and ±5%–6% for trace elements, and for the ICP-MS analyses accuracy is within 2%–12% and precision varies between 1% and 8%.

The whole rock geochemistry of representative plagiogranites and gabbro samples are presented in Tables 1 and 2. A relatively high loss on ignition (LOI) in plagiogranites and gabbros attest to the inconstant degree of alteration. Therefore, the immobile trace elements like Nb, Ti, Zr and V along with REE data (Bonev and Stampfli, 2009) is used for petrogenesis and geochemical signatures.

5. Bulk rock geochemical results

5.1. Plagiogranites

Petrochemical data of plagiogranites (Table 1) show SiO_2 content from 51.81 to 56.71 wt.%, high TiO_2 (1.23–1.83 wt.%) and CaO (3.26–5.67 wt.%), low K_2O (0.08–1.65 wt.%), moderate Al_2O_3 (13.28–14.72 wt.%). The analysis of the plagiogranites reveals that it contains sufficient water, with LOI ranging from 2.42 to 4.50 wt.%. These rocks have higher content of TiO_2, Fe_2O_3 and MgO as compared to continental trondhjemites (Saunders et al., 1979; Jaques and Chappell, 1980). The higher content of Al_2O_3 in the plagiogranites is likely due to plagioclase accumulation. The plagiogranites are subdivided into three groups, i.e. diorites (0–5%), quartz diorites (5–20%), and tonalites/trondhjemites (20–60%) based on the proportion of quartz, K-feldspar and plagioclase (Streckeisen, 1973). In P-Q diagram (after Debon and Le Fort, 1983) and the normative quartz-plagioclase- orthoclase triangular diagram of NOB samples, mostly fall in the quartz diorite field (Figs. 3 and 4). High content of TiO_2 is reflected by the presence of titano-magnetite/ilmenite in the samples. Low content of potassium is an important chemical characteristic in most of the ophiolites. The plagiogranites from NOB differ from the continental trondhjemites by having metalu-

Table 2
Major oxides, trace and REE composition of gabbro from NOB.

Sample	NOL1	NOL8	NOL11	NOL27	NOL31	NOR13	NOR14	NOR15	NOR19	NOR37	NOR42
SiO2	49.94	49.74	48.66	49.77	49.9	47.62	49.63	48.34	49.37	47.66	48.22
TiO2	2.01	2.43	1.94	2.53	2.11	2.18	1.16	1.78	1.83	1.16	1.9
Al2O3	14.34	14.13	14.45	14.34	14.29	13.82	14.66	13.75	13.09	14.44	13.84
Fe2O3t	12.06	13.49	13.35	13.50	12.56	13.63	9.04	12.86	13.09	9.74	12.74
MnO	0.18	0.19	0.2	0.19	0.2	0.17	0.13	0.18	0.17	0.13	0.18
MgO	4.25	3.41	5.23	3.72	4.44	6.54	7	7.36	6.46	9.36	7.19
CaO	6.12	5.62	7.06	5.5	6.15	6.37	9.87	6.33	6.36	8.52	6.39
Na2O	5.14	4.92	4.62	4.97	5.24	4.08	4.58	4.53	4.28	4.07	4.5
K2O	1.11	0.54	0.21	0.67	1.17	0.62	0.4	0.2	0.43	0.19	0.22
P2O5	0.38	0.38	0.24	0.49	0.37	0.19	0.13	0.18	0.23	0.11	0.25
LOI	*2.95*	*3.50*	*2.83*	3.5	3.02	*3.23*	*3.15*	*3.08*	4.26	*3.78*	*3.35*
Total	98.48	98.35	98.79	99.18	99.45	98.45	99.75	98.59	99.57	99.16	98.78
Mg#	45.1	37.1	47.7	39.1	45.2	52.8	64.3	57.2	53.5	69.1	56.8
Ba	412	279	104	220	402	514	191	315	520	163	375
Cr	54	54	41	60	62	39	139	100	120	695	171
V	231	238	249	120	160	317	203	121	160	182	245
Sc	33	33	34	30	35	38	37	37	33	34	41
Co	40	31	38	35	12	51	32	23	33	43	42
Ni	71	58	69	51	57	71	94	62	70	162	91
Cu	94	85	66	50	20	95	108	44	109	115	104
Zn	122	142	91	140	154	123	80	127	125	93	142
Ga	24.67	28.4	25.21	33.1	26.02	22.11	17.97	30.63	22.01	17.62	22.57
Pb	5	4.8	7	4.5	4.7	7.2	4.3	5.9	3.8	3.4	4.3
Th	3.18	7.21	6.5	6.2	6.6	2.94	2.8	7.34	6.2	2.58	3.36
Rb	24	12	4	21	23	13	13	8	12	6	6
U	0.9	0.8	0.75	0.87	0.95	0.8	0.88	0.8	0.88	0.84	0.79
Sr	111	96	68	98	110	273	203	244	204	210	314
Y	30	35	24	48	32	19	15	42	22	12	27
Zr	155	215	154	223	229	98	62	251	60	63	125
Nb	34.9	43.9	30	52	53	18.6	12	52.5	12	12.6	26
La	20	31.5	19.6	33.6	33.2	21.2	14.7	9.5	18.8	23.9	26.4
Ce	38	59.3	37.6	66	65.1	41.6	27.3	18.7	34.3	47.9	52
Pr	4.5	6.9	4.5	8	7.8	5.1	3.3	2.4	4.2	6	6.4
Nd	17.8	27.1	17.5	32.6	33.5	20.7	13.3	10.2	16.6	25	26.5
Sm	4.44	6.33	4.27	7.8	8	5.08	3.41	2.71	4.15	6.14	6.36
Eu	1.55	2.15	1.66	2.54	2.9	1.72	1.34	1.15	1.6	2.05	2.14
Gd	4.96	7.02	4.9	8.73	8.5	5.66	3.55	3.22	4.33	6.95	7.18
Tb	0.75	1.07	0.77	1.35	1.39	0.89	0.55	0.51	0.68	1.08	1.11
Dy	4.27	6.1	4.35	7.54	7.8	4.95	2.94	2.89	3.64	6.05	6.07
Ho	0.79	1.11	0.81	1.46	1.33	0.95	0.6	0.57	0.76	1.15	1.16
Er	1.87	2.73	1.98	3.51	3.6	2.3	1.4	1.36	1.8	2.78	2.75
Tm	0.25	0.38	0.27	0.48	0.3	0.32	0.2	0.19	0.26	0.39	0.38
Yb	1.53	2.35	1.63	2.99	2.8	2.03	1.15	1.13	1.49	2.42	2.36
Lu	0.23	0.34	0.24	0.43	0.44	0.29	0.16	0.16	0.204	0.34	0.33
ΣREE	100.94	154.38	100.08	177.03	176.66	112.79	73.9	54.69	92.81	132.15	141.14
LaN/SmN	2.83	3.13	2.89	2.71	2.61	2.63	2.71	2.21	2.85	2.45	2.61
LaN/YbN	8.81	9.04	8.11	7.58	7.99	7.04	8.62	5.67	8.51	6.66	7.54
Eu/Eu*	1.01	0.99	1.11	0.94	1.08	0.98	1.18	1.19	1.15	0.96	0.97
A/CNK	0.691	0.751	0.700	0.762	0.676	0.727	0.567	0.718	0.684	0.645	0.720

minous character with molecular $Al_2O_3/(CaO + Na_2O + K_2O)$ ratio (mol. A/CNK) < 1.

The studied plagiogranite samples show variable composition in trace elements, but high contents of Th (6.3–9.21 ppm), Co (10–31 ppm), Sc (25–37 ppm) and Cr (38–120 ppm) and low content in Y (38–48 ppm) and Zr (201–290 ppm). The MORB normalization (Pearce, 1983) of the samples shows that there is slight enrichment of Rb, Ba, Th and Nb, are depleted in Ti and Yb (Fig. 5a). The chondrite (Boynton, 1984) normalized (Fig. 5b) REE patterns of the plagiogranite display enrichments in LREE (La_N/Sm_N: 2.37–3.62) and with relatively flat HREE (Eu/Eu*: 0.89–1.06). The REE chondrite normalized pattern is set about 70–200 times chondrite (ΣREE: 92.35–218.1 ppm).

5.2. Gabbro

SiO_2 abundances show a narrow compositional range (Table 2) in the gabbro (47.62–49.94 wt.%) and associated with high TiO_2 (1.16–2.53 wt.%). CaO contents range from 5.5 to 9.87 wt.% and MgO varies from 3.41–9.36 wt.%. With the exception of sample NOR37 where concentrations of Ni and Cr is 162 ppm and 695 ppm, but in the other samples it varies from 51 to 94 ppm in Ni and Cr ranges in 39 to 139 ppm. These concentrations do not meet the requirements for primary mantle melts (Ni > 200 ppm and Cr > 400 ppm), which together with the range of Mg. number (37.1–69.1) in the gabbro implies processes of fractional crystallization. The MORB (Pearce, 1983) normalization of gabbro is characterized by strong enrichment of LILE like Ba (104–520 ppm) and Th (2.58–7.34 ppm) (Fig. 6a). The REE pattern (about 50–100 times) chondrite, (Fig. 6b) is LREE enriched (La_N/Sm_N = 2.21–3.13) and with flat HREE (Eu/Eu*: 0.94–1.19).

6. Discussion

SiO_2-enriched plutonic rocks within the lower oceanic crust, diorites and quartz diorites are believed to be generated by magmatic processes similar to those active in present-day mid-oceanic ridges (e.g. Casey et al., 2007) and supra-subduction zone oceanic basins (e.g. Shervais, 2001). But few others have indicated that plagiogranites may represent partial melts (Malpas, 1979; Amri et al.,

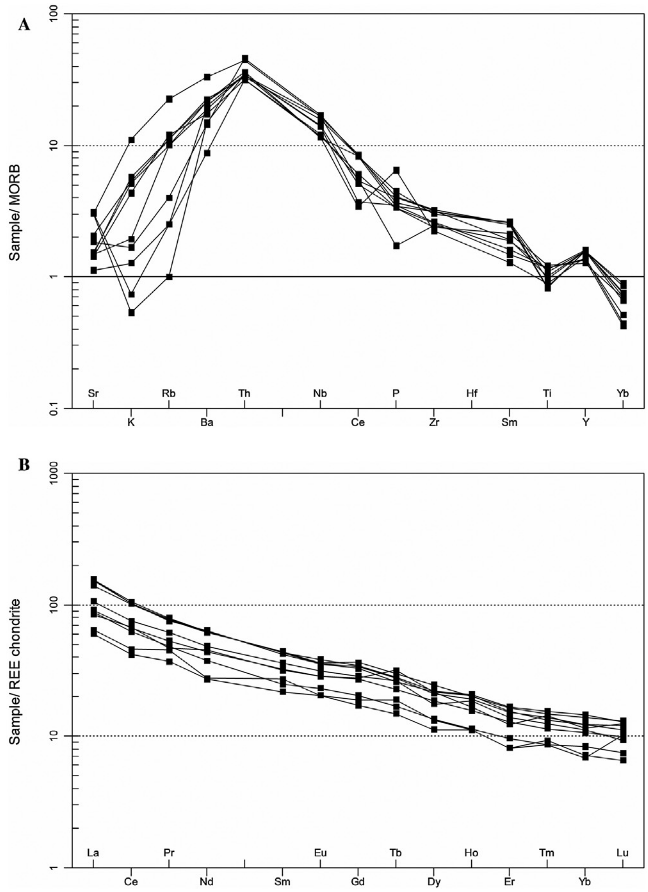

Fig. 5. (a) JPG: MORB normalized of trace element compositions of NOB plagiogranites (after Pearce, 1983). (b) JPG: Chondrite normalized of REE compositions of NOB plagiogranites (Boynton, 1984).

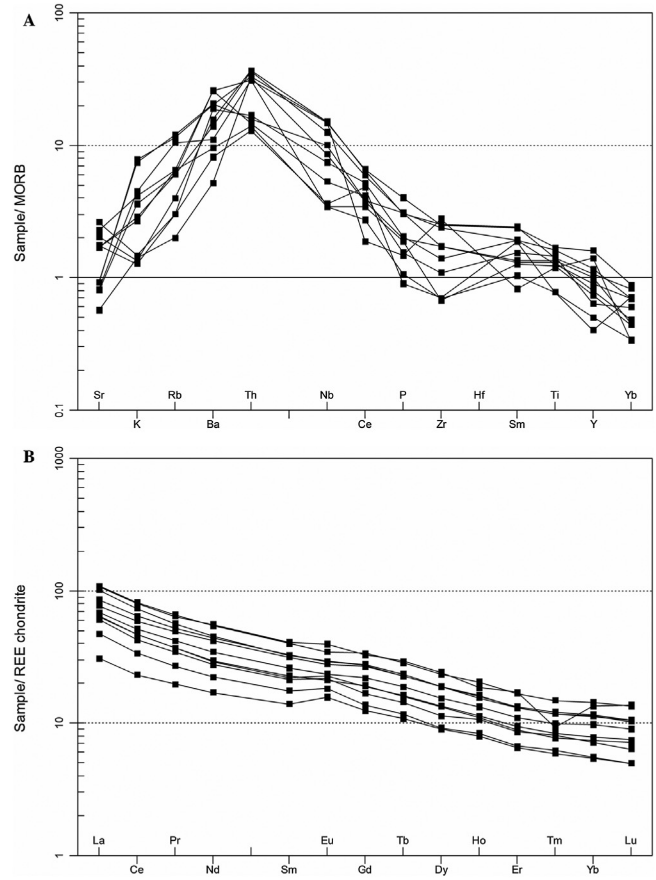

Fig. 6. (a) JPG: MORB normalized of trace element compositions of gabbros (after Pearce, 1983). (b) JPG: Chondrite normalized of REE compositions of gabbros (Boynton, 1984).

1996; Gillis and Coogan, 2002) and thus implies more complex set of processes. Recently Koepke et al. (2004) supported the idea for partial melting hypothesis and have shown that the low pressure melting of hydrated oceanic gabbro produces plagiogranite melts.

The petrogenetic studies of gabbroic and plagiogranites of ophiolites are complicated by post-magmatic structural, mineralogical and chemical changes. Plagiogranites from the ophiolite suite are commonly associated with layered or massive gabbros that occur at the top of the cumulate portion of ophiolites which represent sections of former oceanic crust (Coleman and Donato, 1979; Moores and Vine, 1971). Ophiolite assemblages commonly bear evidences of hydrothermal alteration, due to intensive sea water circulation in sub-seafloor environment (Spooner and Fyfe, 1973; Lecuyer et al., 1990), brecciation and later off-axis metamorphism (Liou and Ernst, 1979). Apart from complex genetic history, there is also the difficulty in sampling of this rock type, but the lower degree of alteration in granitic rocks when compared with mafic rocks counter balances these problems (Pearce et al., 1984).

The existence of myrmekitic texture in these rocks provide textural and chemical evidence for the simultaneous late stage growth of quartz and plagioclase feldspar in an extremely differentiated liquid derived from a low-K magma (Coleman and Donato, 1979). The high Na_2O and low K_2O in gabbro and plagiogranites are due to exchange with sea water or late magmatic vapour-phase transport (Sinton and Byerly, 1980). Melts formed during fractional crystallization experiments using MORB compositions display slightly lower K_2O contents than the melts formed during melting experiments (France et al., 2010). To differentiate between immiscibility, fractional crystallization, and anatexis a ternary plot with $SiO_2/50$-TiO_2-K_2O as apexes can be used and indeed the melts formed during partial melting can reach values exceeding 40% for the K_2O apex and below 20% of the TiO_2 apex. During the lower temperature experiments, the composition of the melt is below the line of saturation for TiO_2 in basaltic melts (Koepke et al., 2007). This can be used to discriminate between gabbro melting (Koepke et al., 2004) and hydrothermally altered dikes melting (Beard and Lofgren, 1991; France et al., 2010) as only hydrothermally altered dikes melts reach silica contents higher than 68 wt% for TiO_2 concentrations <0.5 wt%. Therefore, a combination of TiO_2 versus SiO_2 plot with a ternary plot using $SiO_2/50$-TiO_2-K_2O can be used to discriminate on the origin of natural plagiogranites (France et al., 2010).

A distinctive feature observed in composition during experimental partial melt of hydrated gabbro and diabase is low TiO_2 concentration (<~1 wt%) a diagnostic character of plagiogranite formed through partial melting of mafic crust (France et al., 2010; Koepke et al., 2007). The rocks investigated from NOB contain TiO_2 concentrations above the lower limit for fractional crystallization of MORB (Koepke et al., 2007; Grimes et al., 2013) which is above 1 wt% of TiO_2 (Fig. 7). The ternary plots of AFM and TiO_2-K_2O-$SiO_2/50$ (France et al., 2009b, 2010; France and Nicollet, 2010) indicate that the plagiogranite are tholeiitic in character and gabbro samples are calc-alkaline in nature (Fig. 8). Most of the samples overlap both fractional crystallization of MORB and partial melting of mafic ocean crust. The use of TiO_2 vs SiO_2 diagram and ternary $SiO_2/50$-TiO_2–K_2O diagram can help to discriminate on the plagiogranites origin but these diagrams have to be used with care, these are complementary tools and can be combined with trace element compositions (mainly REE; e.g., Luchitskaya et al., 2005; Bonev and Stampfli, 2009; Brophy, 2008, 2009; Rollinson, 2009).

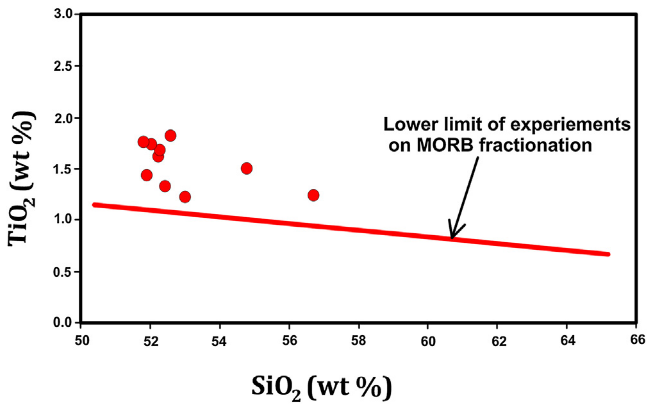

Fig. 7. TIF: Whole rock petrogenetic discrimination (plagiogranite) diagram of TiO_2 vs SiO_2 (Koepke et al., 2007).

So, taking into consideration the behaviour of the trace elements in these rocks is crucial as suggested, the modelling evidence that SiO_2 versus REE systematics should differ for melts formed by fractional crystallization and those formed by hydrous partial melting reactions. The behaviour of REE is sensitive in large part to the presence of amphibole left behind in the residue, during hydrous partial melting. Fractional crystallization produces a positive correlation between concentrations of SiO_2 and REE, whereas hydrous melting produces flat or even decreasing REE trends with increasing SiO_2 for plagiogranite and coexisting mafic crust.

The Harker's diagram of plagiogranites and gabbros from NOB display an increase in K_2O, Yb, ΣREE, La and Zr (Fig. 9) with increasing SiO_2 and decrease in TiO_2, CaO, MgO and Sc with increasing SiO_2. Though Yb vs SiO_2 does not clearly show an increasing trend with SiO_2 but ΣREE and La against silica indicate fractional crystallization rather than hydrous partial melting. The gradual increase of SiO_2, K_2O, ΣREE and Zr from gabbros to plagiogranites reflect that it is generated by relict melt of basaltic magmas. The REE patterns of plagiogranites and gabbros from NOB (Fig. 10) does not overlap, an important evidence to suggest fractional crystallization processes controlled in forming these rocks. The Nidar ophiolite plagiogranites and gabbros is formed through fractional crystallization and can be compared with the REE patterns of NOB plagiogranites and gabbros. But the Nidar ophiolite plagiogranites and gabbros are depleted in LREE with positive and negative Eu anomaly. The increases of $\sum$REE from gabbro (119.69 ppm) to plagiogranites (162.62 ppm) suggest that these rocks derived from common parent magma. The close association of the plagiogranites with gabbros of ophiolites indicates that these rocks are the end products of differentiation of basaltic magma of the ophiolite suites. Number of authors supports the genesis of plagiogranites by fractional crystallization of a basaltic parental magma (e.g. Tiepolo et al., 1997; Borsi et al., 1998; Niu et al., 2002; Montanini et al., 2006). Geochemical data of plagioclase-rich leucocratic rocks (plagiogranite) associated with gabbroic rocks from NOB are comparable with the other ophiolites like Wadi El-Markh Egypt, Oman ophiolite, Nidar Ophiolite Ladakh.

According to Dixon and Rutherford (1983), the amphibole-bearing leucocratic rocks existing in minor amount in the upper part of ophiolitic suites, are perhaps formed by fluid pressure of about 2 kbar, and depth of about 6 km. The geochemical characteristics and the common occurrence of plagiogranites in the uppermost sequences of ophiolites are taken by various workers to be supportive of fractionational crystallization which is also aided by filter-pressing processes. As a result of which the late stage plagiogranite melt intruded the early-crystallized gabbroic rocks (Wildberg, 1987; Rao et al., 2004). Some of the ophiolite complexes are characterized by a notable lack of intermediate compositions between gabbros and the plagiogranites. Dixon and Rutherford (1979) pointed out that such compositional gap ranging maximal from 50 to 60% of SiO_2 could be explained by the process of silicate liquid immiscibility. However, there is no compositional gap (Daly gap; Clague, 1978) observed in NOB. The role of liquid immiscibility to the petrogenesis of plagiogranite is clear by the absence of Fe–Ti-enriched mafic rocks. Immiscible Fe–Ti-enriched mafic rocks related with plagiogranites are known from the Andaman Ophiolite Suite (Shastry et al., 2001) and experimental immiscible liquids (Dixon and Rutherford, 1979). Natural and experimental examples, have high Fe_2O_3 (24–30 wt%) and TiO2 (4.6–8 wt%) concentrations which is well above the values in the NOB gabbros (Table 2). The flat REE pattern without any distinct positive Eu anomaly and enrichment in LREE rules out their origin from the anatexis of amphibolites (Pedersen and Malpas, 1984; Flagler and Spary, 1991). The absence of a negative Eu anomaly in the NOB plagiogranites can be due to elevated Sr and Rb content and also may be due to feldspar accumulation (Birk et al., 1979). There is slight enrichment in LREE of NOB plagiogranite in contrast to the plagiogranites from Troodos Massif and Semail Nappe that are depleted in LREE relative to HREE, showing low K-tholeiitic patterns. The plot Cr vs Y (after Pearce, 1982) indicates MORB setting (Fig. 11). The petrogra-

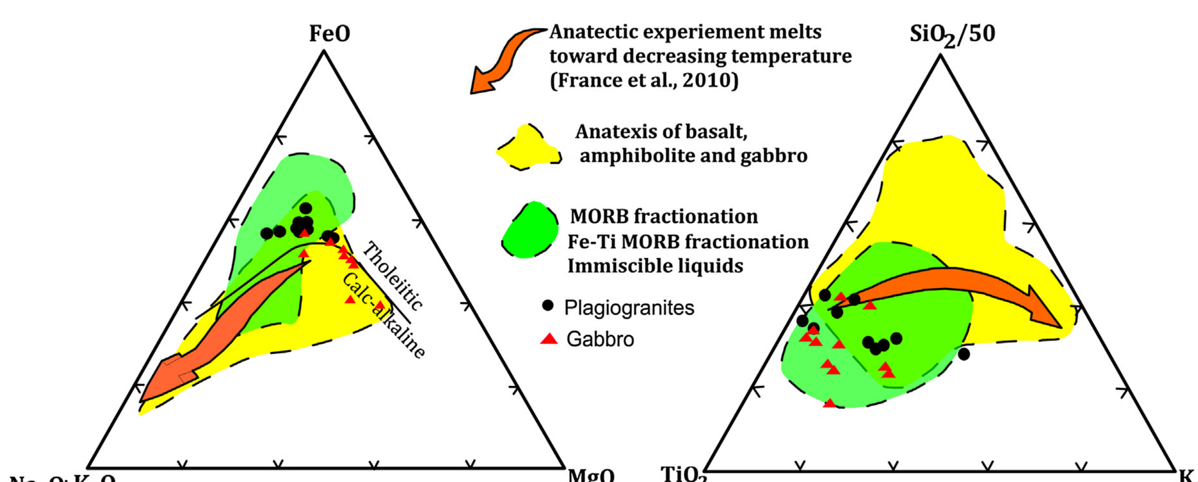

Fig. 8. TIF: Triangular diagrams; a) A (Na_2O+K_2O)-FeO-MgO discrimination for tholeiitic and calc-alkaline series (Irvine and Baragar, 1971); b) Si_2O/50-TiO_2-K_2O ternary plot for plagiogranite origin (France et al., 2009b, 2010; France and Nicollet, 2010).

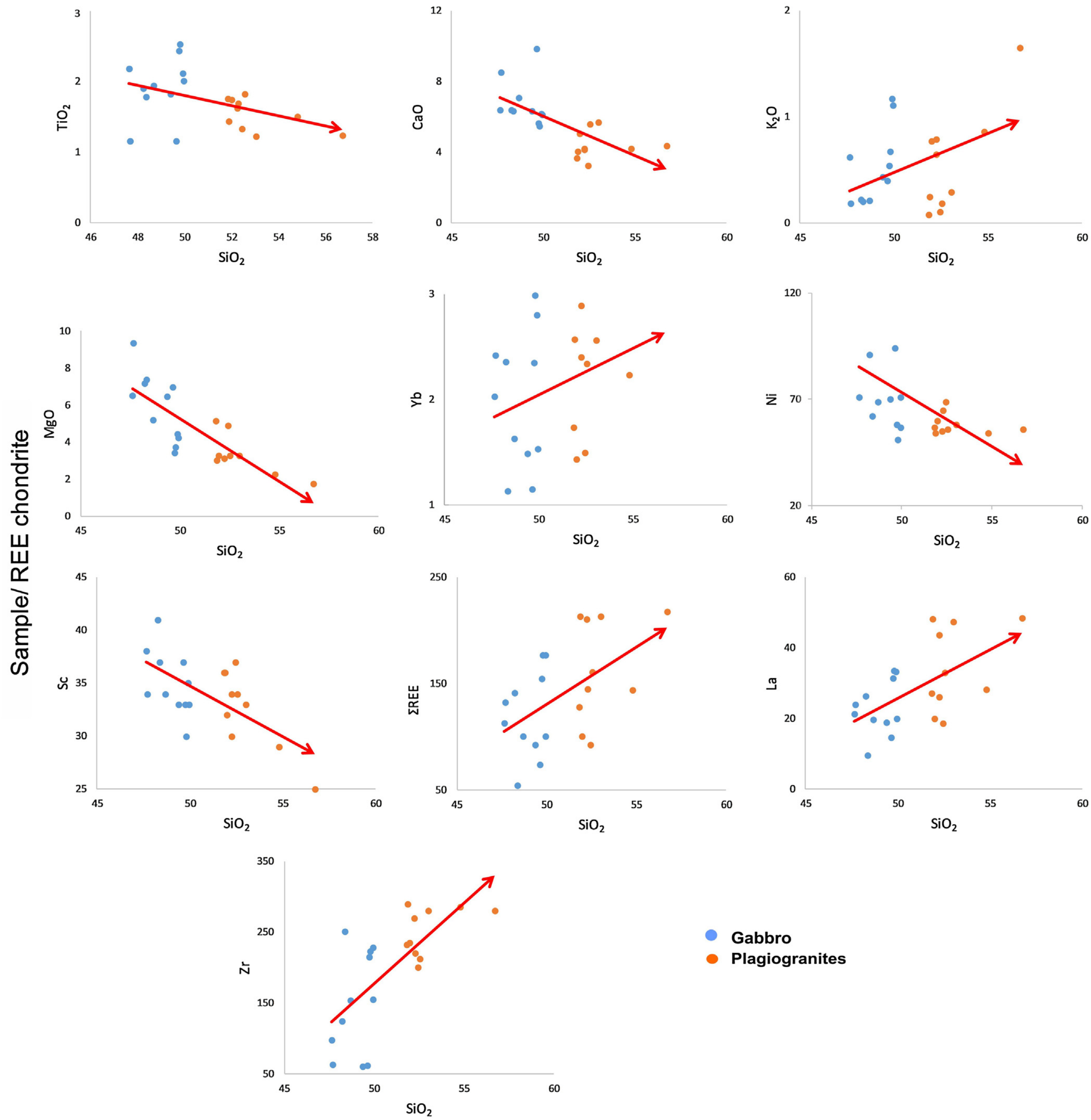

Fig. 9. JPG: Harker's variation diagram of gabbro and plagiogranites from NOB.

phy and the REE patterns of the NOB plagiogranites show that they are distinctive magmatic rocks related with ophiolitic complexes, as similarly observed in other ophiolites.

7. Conclusion

- Petrographic observations, major-element and trace element data of the NOB plagiogranites and their intrusive nature with host gabbroic rocks observed in the field suggest that the plagiogranites were produced by fractional crystallization. Plagiogranites from NOB are the products of differentiation with residual melts for the generation of plagiogranites after extensive crystallization of subalkaline tholeiitic magma.
- The average increase of SiO_2, K_2O, Y and Zr values from gabbros towards plagiogranite and the intergrowths of plagioclase and quartz in plagiogranites reveal that the plagiogranites are generated by a relict melt which is cogenetic with gabbros and they form a rational fractional trend.
- The geochemical behaviour of NOB gabbros and plagiogranites indicates that these rocks originated from fractional crystallization of basaltic parental magmas at MOR.

Acknowledgements

This paper is part of first author's PhD Thesis and the authors acknowledge Nagaland University. The lead author acknowledges

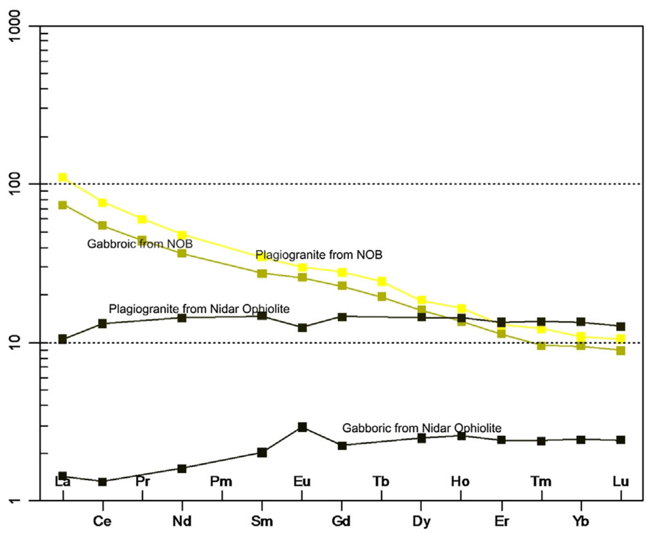

Fig. 10. JPG: Chondrite normalized of REE compositions of NOB and Nidar ophiolite plagiogranites (Boynton, 1984).

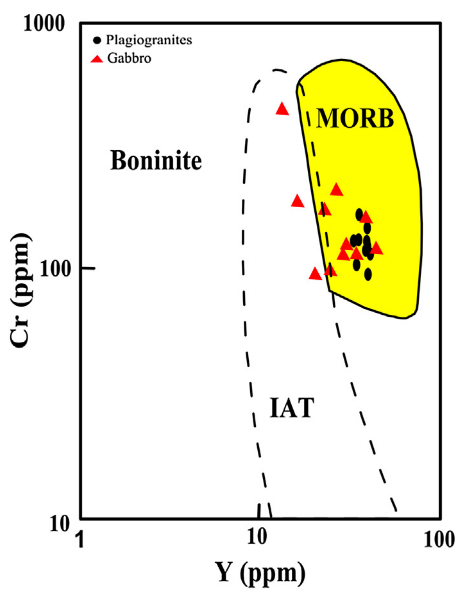

Fig. 11. TIF: Plot of plagiogranite and gabbros samples from NOB on Cr vs Y discrimination diagram (after Pearce, 1982).

the financial support of the scientific research project of DST as Fast Track Young Scientist (SR/FTP/ES-60/2014). Very helpful and constructive reviewers by Nilanjan Chatterjee and anonymous reviwers are gratefully acknowledged.

References

Agrawal, O.P., Ghose, N.C., 1986. Geology and stratigraphy of the Naga Hills ophiolite between Meluri and awankhoo Phek district, Nagaland, India. In: Ghose, N.C., Varadarajan, S. (Eds.), Ophiolite and Indian Plate Margin. Sumna Publishers, Patna, pp. 163–195.
Agrawal, O.P., Kacker, R.N., 1980. Nagaland ophiolites, India—a subduction zone ophiolite complex in a Tethyan orogenic belt. In: Abstracts of the International Ophiolite Symposium, Cyprus, pp. 454–461.
Alabaster, T., Pearce, J.A., Malpas, J., 1982. The volcanic stratigraphy and petrogenesis of the Oman ophiolite complex. Contrib. Miner. Petrol. 81, 168–183.
Amri, I., Benoit, M.Y., Ceuleneer, G., 1996. Tectonic setting for the genesis of oceanic plagiogranites: evidence from a paleospreading structure in the Oman ophiolite. Earth Planet. Sci. Lett. 139, 177–194.
Aumento, F., 1969. Diorites from the mid-Altanic ridge at 45°N. Science 165, 1112–1113.
Beard, J.S., Lofgren, G.E., 1991. Dehydration melting and water saturated melting of basaltic and andesitic greenstones and amphibolites at 1, 3, and 6.9 kb. J. Petrol. 32, 365–401.
Bhattacharjee, C.C., 1991. The Ophiolites of Northeast India—a subduction zone ophiolite complex of the Indo-Burman Orogenic belt. Tectonophysics 191, 213–222.
Birk, D., Koljonen, J., Rosenberg, R.J., 1979. Rare earth distribution in Archean granitoid plutons of the Wabigoon volcanic-plutonic belt, north western Ontario. Can. J. Earth Sci. 16, 270–289.
Bonev, N., Stampfli, G., 2009. Gabbro, plagiogranite and associated dykes in the supra-subduction zone Evros Ophiolites north eastern Greece. Geol. Mag. 146, 72–91.
Borsi, L., Petrini, R., Cortesogno, L., Gaggero, L., Crispini, L., 1998. Modelling of plagiogranite genesis and implications for the evolution of the Ligurian-Piedmont oceanic basin (Ligurian Alps, Italy). Neues Jahrbuch fur Mineralogie Monatshefte 5, 208–220.
Boynton, W.V., 1984. Geochemistry of the rare earth elements: meteorite studies. In: Henderson, P. (Ed.), Rare Earth Element Geochemistry. Elsevier, pp. 63–114.
Brophy, J.G., 2008. A study of rare earth element (REE)-SiO_2 variations in felsic liquids generated by basalt fractionation and amphibolite melting: a potential test for discriminating. Contrib. Miner. Petrol. 156, 337–357, http://dx.doi.org/10.1007/s00410-008-0289-x.
Brophy, J.G., 2009. La-SiO2 and Yb-SiO2 systematics in mid-ocean ridge magmas: implications for the origin of oceanic plagiogranite. Contrib. Miner. Petrol. 158, 99–111.
Casey, J.F., Banerji, D., Zarian, P., 2007. Leg 179 synthesis: geochemistry, stratigraphy, and structure of gabbroic rocks drilled in ODP Hole 1105A, Southwest Indian Ridge. In: Casey, J.F., Miller, D.J. (Eds.), Proceed. ODP Sci. Results vol. 179, 1–125, http://dx.doi.org/10.2973/odp.proc.sr.179.001.2007.
Casey, J.F., 1997. Comparsion of major and trace-element geochemistry of abyssal peridotites and mafic plutonic rocks with basalts from the MARK region of the mid-Altantic ridge. In: Karsen, J.A., Cannat, M., Miller, D.J., Elthon, D. (Eds.), Proceeding of the ODP, Science Research, 153. Ocean Drilling Program College Station, 181–241.
Chattopadhyay, B., Venkataramana, P., Roy, D.K., Bhattacharya, S., Ghose, S., 1983. Geology of Naga Hills ophiolite. Rec. Geol. Surv. India 112, 59–115.
Clague, D.A., 1978. The oceanic basalt-trachyte association: an explanation of the Daly gap. J. Geol. 86, 739–743.
Coleman, R.G., Donato, M.M., 1979. Oceanic plagiogranite revisited. In: Barker, F. (Ed.), Trondhjemites, Dacites, and Related Rocks. Elsevier, Amsterdam, pp. 149–167.
Coleman, R.G., Peterman, Z.E., 1975. Oceanic plagiogranite. J. Geophys. Res. 80, 1099–1108.
Debon, F., Le Fort, P., 1983. A chemical-mineralogical classification of common plutonic rocks and associations. Trans. R. Soc. Edinburgh Earth Sci. 73, 135–149.
Dick, H.J.B., Bullen, T., 1984. Chromian spinel as a petro genetic indicator in abyssal and alpine-type peridotites and spatially associated lavas. Contrib. Mineral. Petrol. 86, 54–76.
Dick, H.J.B., Natland, J.H., Alt, J.C., Bach, W., Bideau, D., Gee, J.S., Haggas, S., Hertogen, J.G.H., Hirth, G., Holm, P.M., Ildefonse, B., Iturrino, G.J., John, B.E., Kelley, D.S., Kikawa, E., Kingdon, A., LeRoux, P.J., Maeda, J., Meyer, P.S., Miller, D.J., Naslund, H.R., Niu, Y.L., Robinson, P.T., Snow, J., Stephen, R.A., Trimby, P.W., Worm, H.U., Yoshinobu, A., 2000. A long in situ section of the lower ocean crust: results of ODP Leg 176 drilling at the Southwest Indian Ridge. Earth Planet. Sci. Lett. 179, 31–51.
Dilek, Y., Flower, M.F.J., 2003. Arc-trench roll-back and forearc accretion: 2. A model template for ophiolites in Albania, Cyprus, and Oman. In: Dilek, Y., Robinson, P.T. (Eds.), Ophiolites in Earth History, vol. 218. Geol. Soc. Lond. Spec. Pub., pp. 43–68.
Dixon, S.J., Rutherford, M.J., 1979. Plagiogranites as late-stage immiscible liquids in ophiolite and mid-ocean ridge suites: an experimental study. Earth Planet. Sci. Lett. 45, 45–60.
Dixon, S.S., Rutherford, M.J., 1983. The origin of rhyolite and plagiogranite in oceanic crust: an experimental study. J. Petrol. 24, 1–25.
Engel, C.G., Fisher, R.L., 1975. Granitic to ultramafic rock complexes of the Indian Ocean ridge system, Western Indian Ocean. Geol. Soc. Am. Bull. 86, 1553–1578.
Flagler, P.A., Spary, J.G., 1991. Generation of oceanic plagiogranites by amphibolite anatexis in oceanic shear zones. Geology 19, 70–73.
Floyd, P.A., Yalınız, M.K., Göncüolu, M.C., 1998. Geochemistry and petrogenesis of intrusive and extrusive ophiolitic plagiogranites Central Anatolian Crystalline Complex, Turkey. Lithos 42, 225–241.
France, L., Nicollet, C., 2010. MetaRep. an extended CMAS 3D program to visualize mafic (CMAS, ACF-S, ACF-N), and pelitic (AFM-K AFM-S, AKF-S) projections. Comput. Geosci. 36, 786–791.
France, L., Ouillon, N., Chazot, G., Kornprobst, J., Boivin, P., 2009b. CMAS 3D, a new program to visualize and project major elements compositions in the CMAS system. Comput. Geosci. 35, 1304–1310.
France, L., Koepke, J., Ildefonse, B., Cichy, S.B., Deschamps, F., 2010. Hydrous partial melting in the sheeted dike complex at fast spreading ridges: experimental and natural observations. Contrib. Miner. Petrol. 160, 683–704.
Gerlach, D.C., Leeman, W.P., Aveí Lallemant, H.G., 1981. Petrology and geochemistry of plagiogranite in the Canyon Mountain ophiolite, Oregon. Contrib. Miner. Petrol. 72, 82–92.
Ghose, N.C., Agrawal, O.P., 1989. Geological framework of the central part of Naga Hills. In: Ghose, N.C. (Ed.), Phanerozoic Ophiolites of India and Associated Mineral Resources. Sumna Publications, Patna, pp. 165–188.

Ghose, N.C., Agrawal, O.P., Chatterjee, N., 2010. A geological and mineralogical study of eclogite and glaucophane schists in the Naga Hills Ophiolite, Northeast India. Isl. Arc 19, 336–356.

Ghose, N.C., Chatterjee, N., Fareeduddin, 2014. A Petrographic Atlas of Ophiolite—An Example from the Eastern India—Asia Collision. Springer, Heidelberg, 25.

Gillis, K.M., Coogan, L.A., 2002. Anatectic migmatites from the roof of an ocean ridge magma chamber. J. Petrol. 43, 2075–2095.

Grimes, Craig B., Ushikubo, T., Kozdon, R., Valley, J.W., 2013. Perspectives on the origin of plagiogranite in ophiolite from oxygen isotope in zircon. Lithos 179, 48–66.

Irvine, T.M., Baragar, W.R., 1971. A guide to the chemical classification of common volcanic rocks. Can. J. Earth Sci. 8, 523–548.

Jaques, A.C., Chappell, D.W., 1980. Petrology and geochemistry of Papuan ultramafic belt. Contrib. Miner. Petrol. 75, 55–70.

Koepke, J., Feig, S.T., Snow, J., Freise, M., 2004. Petrogenesis of oceanic plagiogranites by partial melting of gabbros: an experimental study. Contrib. Miner. Petrol. 146, 414–432.

Koepke, J., Berndt, J., Feig, S.T., Holtz, F., 2007. The formation of SiO_2-rich melts within the deep oceanic crust by hydrous partial melting of gabbros. Contrib. Miner. Petrol. 153, 67–84.

Lecuyer, C., Brouxel, M., Albarede, F., 1990. Elemental fluxes hydrothermal alteration of the Trinity ophiolite (Caledonian, U.S.A) by sea water. Chem. Geol. 89, 87–115.

Liou, J.G., Ernst, W.G., 1979. Ocean ridge metamorphism of the east Taiwan ophiolite. Contrib. Miner. Petrol. 68, 335–348.

Luchitskaya, M.V., Morozov, O.L., Palandzhyan, S.A., 2005. Plagiogranite magmatism in the Mesozoic island-arc structure of the Pekulney Ridge, Chukotka Peninsula, NE Russia. Lithos 79, 251–269, http://dx.doi.org/10.1016/j.lithos.2004.04.056.

Malpas, J., 1979. Two contrasting trondhjemite associations from transported ophiolites in Western Newfoundland: initial report. In: Barker, F. (Ed.), Trondhjemites, Dacites, and Related Rocks. Elsevier, Amsterdam, pp. 465–487.

Montanini, A., Travaglioli, M., Serri, G., Dostal, J., Ricci, C.A., 2006. Petrology of gabbroic to plagiogranitic rocks from southern Tuscany (Italy): evidence for magmatic differentiation in a ophiolite sequence. Ofioliti 31, 55–69.

Moores, E.M., Vine, F.J., 1971. The Troodos massif, Cyprus and other ophiolites as oceanic crust—evaluation and implications. Philos. Trans. R. Soc. Lond. 268, 443–466.

Niu, Y., Gilmore, T., Mackie, S., Greig, A., Bach, W., 2002. Mineral chemistry, whole-rock compositions, and petrogenesis of Leg 176 gabbros: data and discussion. In: Natland, J.H., Dick, H.J.B., Miller, D.J., Von Herzen, R.P. (Eds.), Proceedings of ODP, Scientific Results. 176. Ocean Drilling Program. College Station, TX, pp. 1–60 ([Online] http://wwwodp.tamu.edu/publications/176_SR/VOLUME/CHAPTERS/SR76_08.PDF).

Pallister, J.S., Knight, R.J., 1981. Rare-earth element geochemistry of the Samail ophiolite near Ibra, Oman. J. Geophys. Res. 86, 2673–2691.

Pearce, J.A., Alabaster, T., Shelton, A.W., Searle, M.P., 1981. The Oman ophiolite as a Cretaceous arc-basin complex: evidence and implications. Philos. Trans. R. Soc. Lond. 300, 299–317.

Pearce, J.A., Harris, N.B., Tindle, A.G., 1984. Trace element discrimination diagrams for the tectonic interpretation of granitic rocks. J. Petrol. 25, 956–983.

Pearce, J.A., 1982. Trace element characteristics of lavas from destructive plate boundaries. In: Thorpe, R.S. (Ed.), Orogenic Andesites. Wiley, Chichester, pp. 528–548.

Pearce, J.A., 1983. Role of the sub-continental lithosphere in magma genesis at active continental margins. In: Hawkesworth, C.J., Norry, M.J. (Eds.), Continental Basalts and Mantle Xenoliths. Shiva Publishing, Nantwich, UK, pp. 230–249.

Pedersen, R.B., Malpas, J., 1984. The origin of oceanic plagiogranites from the Karmoy ophiolite, western Norway. Contrib. Miner. Petrol. 88, 36–52.

Philpotts, A.R., 1976. Silicate liquid immiscibility: its probable extent and petrogenetic significance. Am. J. Sci. 276, 1147–1177.

Rao, D. Rameshwar, Rai, Hakim, Kumar, J. Senthil, 2004. Origin of oceanic plagiogranite in the Nidar ophiolite sequence of eastern Ladakh, India. Curr. Sci. 87, 999–1004.

Razaei, Z., Noghreyan, M., Khalili, M., 2012. Petrological study of plagiogranites in the Nain ophiolite (Central Iran). Ofioliti 37, 93–99.

Robertson, A.H.F., 2002. Overview of the genesis and emplacement of Mesozoic ophiolites in the Eastern Mediterranean Tethyan region. Lithos 65, 1–67.

Rollinson, H., 2009. New models for the genesis of plagiogranites in the Oman ophiolite. Lithos 112, 603–614.

Saunders, A.D., Tarney, J., Stern, C.R., Dalziel, I.W.D., 1979. Geochemistry of Mesozoic marginal basin floor igneous rocks from southern Chile. Geol. Soc. Am. Bull. 90, 237–258.

Schroetter, J.M., Pagé, P., Bédard, J.H., Tremblay, A., Bécu, V., 2003. Forearc extension and sea-floor spreading in the Thetford-Mines Ophiolite Complex. In: Dilek, Y., Robinson, P.T. (Eds.), Ophiolites in Earth History, vol. 218. Geol. Soc. Lond. Spec. Pub., pp. 231–251.

Shastry, A., Srivasatva, R.K., Chandra, R., Genner, G.A., 2001. Fe-Ti-enriched mafic rocks from south Andaman ophiolite suite: implication of late stage liquid immisicibilty. Curr. Sci. 80, 453–454.

Shervais, J.W., 2001. Birth, death, and resurrection: the life cycle of suprasubduction zone ophiolites. Geochem. Geophys. Geosyst. 2, 2001, http://dx.doi.org/10.1029/2000GC000080.

Silantyev, S.A., 1998. Origin conditions of the mid-Atlantic Ridge plutonic complex at 13°–17°N. Petrology 6, 381–421.

Singh, A.K., Nayak, Ranjit, Khogenkumar, S., Subramanyam, K.S.V., Thakur, S.S., Singh, B.R.K., Satyanarayanan, M., 2016. Genesis and tectonic implications of cumulate pyroxenites and tectonite peridotites from the Nagaland–Manipur ophiolites, Northeast India: constraints from mineralogical and geochemical characteristics. Geol. J. http://doi.org/101002/gj.2769.

Sinton, J.M., Byerly, G.R., 1980. Silicic differentiates of abyssal oceanic magmas: evidence for late-magmatic vapour transport of potassium. Earth Planet. Sci. Lett. 47, 423–430.

Spooner, E.T.C., Fyfe, W.S., 1973. Sub-sea-floor metamorphism, heat and mass transfer. Contrib. Miner. Petrol. 42, 287–304.

Spulber, S.D., Rutherford, M.J., 1983. The origin of rhyolite and plagiogranite in oceanic crust: an experimental study. J. Petrol. 24, l–25.

Stern, R.J., Bloomer, S.H., 1992. Subduction zone infancy: examples from the Eocene Izu-Bonin-Mariana and Jurassic California arcs. Geol. Soc. Am. Bull. 104, 1621–1636, http://dx.doi.org/10.1130/0016-7606(1992)104<1621:SZIEFT>2.3.CO;2.

Streckeisen, A., 1973. Plutonic rocks: classification and nomenclature recommended by the IUGS Subcommission on the systematics of igneous rocks. Geotimes 18, 26–30.

Tiepolo, M., Tribuzio, R., Vannucci, R., 1997. Mg- and Fe-gabbroids from Northern Apennine ophiolites: parental liquids and igneous differentiation process. Ofioliti 22, 57–69.

Tremblay, A., Meshi, A., Bédard, J.H., 2009. Oceanic core complexes and ancient oceanic lithosphere: insights from Iapetan and Tethyan ophiolites (Canada and Albania). Tectonophysics 473 (1–2), 36–52, http://dx.doi.org/10.1016/j.tecto.2008.08.003.

Tremblay, A., Ruffet, G., Bédard, J.H., 2011. Obduction of Tethyan-type ophiolites-a case-study from the Thetford-mines ophiolitic complex Quebec Appalachians, Canada. Lithos 125, 10–26.

Venkataramana, P., Datta, A.K., Acharyya, S.K., 1986. Petrography and petrochemistry. In geology of Nagaland ophiolite. Mem. Geol. Surv. India 119, 33–63.

Wildberg, H.G.H., 1987. High level and low level plagiogranites from the Nicoya ophiolite complex, Costa Rica, Central America. Geol. Rundsch. 76, 285–301.